1521-009X/44/10/1569–1578$25.00
Drug Metabolism and Disposition

http://dx.doi.org/10.1124/dmd.116.071639
Drug Metab Dispos 44:1569–1578, October 2016

The Use of In Vitro Data and Physiologically-Based Pharmacokinetic Modeling to Predict Drug Metabolite Exposure: Desipramine Exposure in Cytochrome P4502D6 Extensive and Poor Metabolizers Following Administration of Imipramine

Hoa Q. Nguyen, Ernesto Callegari, and R. Scott Obach

Department of Pharmacokinetics, Dynamics, and Metabolism, Pfizer Global Research and Development, Groton, Connecticut

Received May 18, 2016; accepted July 18, 2016

ABSTRACT

Major circulating drug metabolites can be as important as the drugs themselves in efficacy and safety, so establishing methods whereby exposure to major metabolites following administration of parent drug can be predicted is important. In this study, imipramine, a tricyclic antidepressant, and its major metabolite desipramine were selected as a model system to develop metabolite prediction methods. Imipramine undergoes N-demethylation to form the active metabolite desipramine, and both imipramine and desipramine are converted to hydroxylated metabolites by the polymorphic enzyme CYP2D6. The objective of the present study is to determine whether the human pharmacokinetics of desipramine following dosing of imipramine can be predicted using static and dynamic physiologically-based pharmacokinetic (PBPK) models from in vitro input data for CYP2D6 extensive metabolizer (EM) and poor metabolizer (PM) populations. The intrinsic metabolic clearances of parent drug and metabolite were estimated using human liver microsomes (CYP2D6 PM and EM) and hepatocytes. Passive diffusion clearance of desipramine, used in the estimation of availability of the metabolite, was predicted from passive permeability and hepatocyte surface area. The predicted area under the curve (AUC_m/AUC_p) of desipramine/imipramine was 12- to 20-fold higher in PM compared with EM subjects following i.v. or oral doses of imipramine using the static model. Moreover, the PBPK model was able to recover simultaneously plasma profiles of imipramine and desipramine in populations with different phenotypes of CYP2D6. This example suggested that mechanistic PBPK modeling combined with information obtained from in vitro studies can provide quantitative solutions to predict in vivo pharmacokinetics of drugs and major metabolites in a target human population.

Introduction

Recent regulatory guidance from the Food and Drug Administration and International Council for Harmonisation (Guideline, 2009; http://www.fda.gov/ucm/groups/fdagov-public/@fdagov-drugs-gen/documents/document/ucm079266.pdf) proposes that any drug metabolite with exposure >10% of the parent or of the total drug-related material exposure at steady state in humans warrants further consideration with regard to safety. These guidelines recommend identifying the metabolic profile of the drug in humans, and determining systemic exposure of relevant metabolite (m) area under the concentration-time curve (AUC) relative to parent (p) AUC (AUC_m/AUC_P) in clinical and nonclinical studies. The metabolite/parent area under the plasma concentration versus time curve ratio (AUC_m/AUC_p) is also a commonly used metric in drug interaction studies involving metabolites (Yeung et al., 2011; European Medicines Agency, 2012; Food and Drug Administration, 2012; Callegari et al., 2013; Yu and Tweedie, 2013).

The establishment of drug metabolite kinetic principles dates back to the 1980s (Houston, 1981; Houston and Taylor, 1984; Pang, 1985; St-Pierre et al., 1988). However, although the use of in vitro studies to predict in vivo pharmacokinetics of drugs is commonplace, the use of these approaches to predict pharmacokinetics of metabolites has not been thoroughly established due to the number of contributing variables on metabolite exposure. The equations developed by Houston (1981) for the metabolite/parent ratio (AUC_m/AUC_p) represent static models, which provide conceptual insight as to the determinants of metabolite exposure, including the clearance rate of the parent drug, the fraction of the dose of the parent drug that is converted to the metabolite, and the subsequent clearance of the metabolite. Another factor that can also impact metabolite disposition is its systemic availability following formation from parent drug, which depends upon sequential elimination, permeability, and transport properties of the metabolite.

A different approach to the understanding of circulating metabolite in vivo pharmacokinetic (PK) behavior is utilizing in vitro data of parent

H.Q.N. is a Pfizer Worldwide Research and Development Postdoctoral Fellowship awardee.

dx.doi.org/10.1124/dmd.116.071639.

ABBREVIATIONS: AUC, area under the concentration-time curve; CL_{int}, intrinsic clearance; $CL_{int,pass}$, unbound passive diffusion CL_{int}; $CL_{int,u,met}$, unbound metabolic CL_{int}; CL_m, total clearance of the metabolite; CL_{int2}, intrinsic clearance representing high K_m site; CL_p, total clearance of the parent drug; EM, extensive metabolizer; $f_{CL,m}$, fraction of the clearance of the parent drug that yields the metabolite; F_h, hepatic first-pass availability; f_m, fractional conversion from parent drug; F_m, systemic availability; fu_B, free fraction in blood; fu_{cell}, fraction unbound in hepatocytes; fu_p, fraction unbound in plasma; HLM, human liver microsome; HPLC, high-performance liquid chromatography; IS, internal standard; Km, Michaelis-Menten constant; m, metabolite; MS, mass spectrometry; m/z, mass/charge ratio; p, parent; PK, pharmacokinetics; PBPK, physiologically-based pharmacokinetic; PM, poor metabolizer; Q_h, hepatic blood flow; $t_{1/2}$, half life; UHPLC, ultra-high performance liquid chromatography; V_{max}, maximal reaction velocity; V_{ss}, volumes of distribution at steady state.

TABLE 1

Parameters for imipramine and active metabolite desipramine in PBPK model

Parameter	Imipramine	Desipramine	Source
Molecular weight (g/mol)	280.4	266.4	ACD
logP	4.8	4.57	ACD
Compound type	Base	Base	ACD
pK_a	9.45	10.26	ACD
B/P	1.02	1.16	(Ciraulo et al., 1988)
$f_{u,p}$	0.26	0.21	Measured
Absorption			
Model	First-order	n/a	
Fraction absorbed	1	n/a	(Sallee and Pollock, 1990)
k_a (h^{-1})	1	n/a	Simcyp default
$f_{u,gut}$	1	n/a	Assumed
MDCK-II (10^{-6} cm/s)	39.3	n/a	(Mahar Doan et al., 2002)
Distribution			
Model	Minimal PBPK	Minimal PBPK	
V_{ss} (L/kg)	11	6.5	Predicted using method 2 (Rodgers and Rowland, 2006)
Elimination			
Enzyme kinetics (CL_{int}) (μL/min/mg protein)	9.12	22	Measured
Additional CL (Hep CL_{int}) (μL/min/10^6 cells)	8	0	Measured
fu_{mic}	0.42	0.39	Measured
Renal clearance (L/hr)	0.15	1.0	(Ciraulo et al., 1988)

ACD, values calculated using Advanced Chemistry Development (ACD/Laboratories) Software V12.5; CL, clearance; $f_{u,gut}$, Free fraction of substrate in the enterocyte; k_a, Absorption rate constant; MDCK-II, Madin-Darby canine kidney; n/a, not applicable.

drug and metabolites in integrated dynamic physiologically-based pharmacokinetic (PBPK) models. PBPK is also potentially of value as a tool to evaluate the effect of various population factors on pharmacokinetic outcomes, including genetic polymorphism (Jamei et al., 2009; Rowland et al., 2011; Vieira et al., 2014).

In the present study, desipramine, an active metabolite of the tricyclic antidepressant imipramine, was selected as a test case to apply the approach of integrating in vitro data into static and dynamic PBPK models for metabolite exposure prediction following administration of parent drug, which was proposed in the previous study (Nguyen et al., 2016). Both imipramine and desipramine were demonstrated to undergo hydroxylation catalyzed by CYP2D6 (Brøsen and Gram, 1988; Sallee and Pollock, 1990). The differences in PK, due to variability in expression of CYP2D6, may lead to clinically significant differences in the treatment of depression with desipramine and imipramine (Dahl et al., 1992; Furman et al., 2004; Schenk et al., 2008). In this study, the impact of CYP2D6 polymorphism on metabolism and disposition of both parent drug and metabolite was investigated by simulating time-course profiles in populations of CYP2D6 extensive metabolizer (EM) and poor metabolizer (PM) genotypes. In vitro data were generated for imipramine and desipramine, including metabolic intrinsic clearance (CL_{int}), protein binding, and membrane permeability. These data were used as input values for static and PBPK models in CYP2D6 EM and PM subjects, and compared with the PK parameters reported in the literature.

Materials and Methods

Materials

Imipramine, desipramine, and amitriptyline hydrochloride were purchased from Sigma-Aldrich (St. Louis, MO). Pooled human liver microsomes (HLMs;

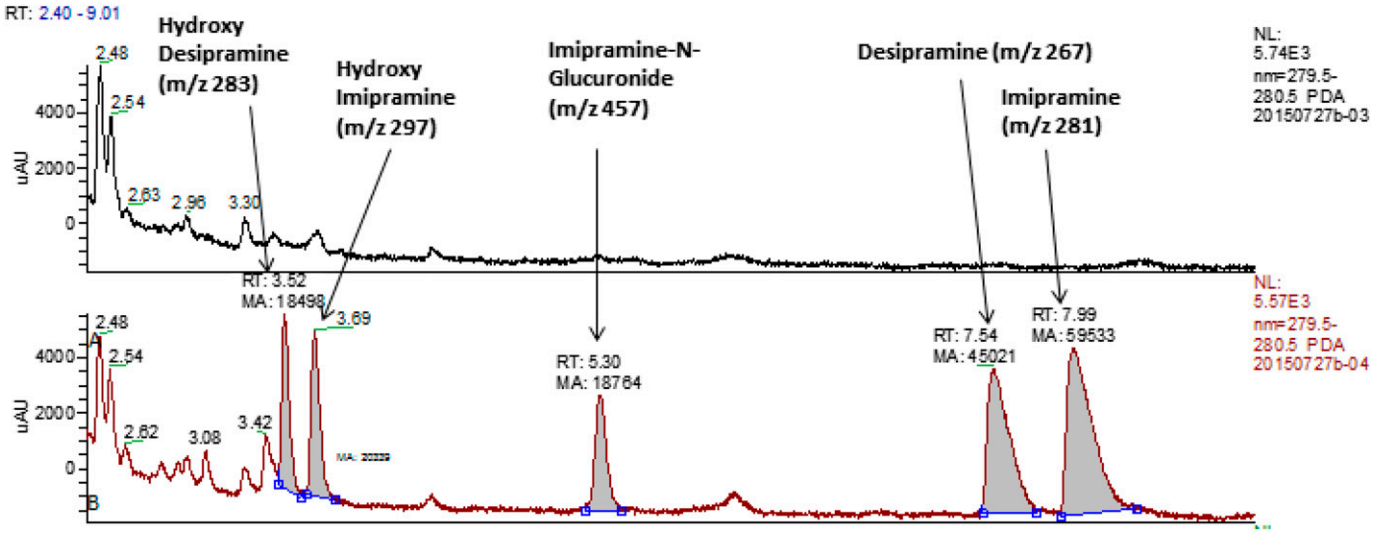

Fig. 1. HPLC-UV traces of extracts of human hepatocyte incubations of imipramine. The trace on the top is the UV chromatogram of the control incubation without parent drug. The trace on the bottom is the UV chromatogram of imipramine incubation.

lot number HLM102, a mixture of both genders, CYP2D6 EM phenotype) were prepared under contract from BD Biosciences (Woburn, MA). CYP2D6 PM HLMs (lot HH35, HH79, 413, 499, and 486) were purchased from BD Gentest (Woburn, MA) and Xenotech (Lenexa, KS) and pooled. Cryopreserved human hepatocytes (N = 10 donors, mixed gender) were purchased from Celsis IVT (Baltimore, MD). Other reagents and solvents used were from standard suppliers and were of reagent or high-performance liquid chromatography (HPLC) grade.

Metabolite Profile of Imipramine in Hepatocytes

In Vitro Incubation. Human hepatocyte (~0.75 × 10^6 cells/mL) incubations were performed in Williams E medium in a total volume of 1 mL using 10 μM imipramine concentration. Incubations were conducted at 37°C under a gas mixture of 5% CO_2/95% O_2. At time zero, 500 μL sample was quenched with 2.5 mL acetonitrile. At time 30 and 60 minutes, 250 μL sample at each time was added to the same volume of 2.5 mL acetonitrile. The precipitate was removed by centrifugation (1700g) for 5 minutes, the supernatant was decanted into a 15-mL conical glass tube, and the liquid was evaporated under a vacuum at 35°C using Genevac evaporator. The resulting residue was reconstituted in 0.1 mL water containing 1% formic acid for HPLC-UV- tandem mass spectrometry analysis.

Metabolite Identification. The imipramine human hepatocyte extracts were analyzed by Ultra-High Performance Liquid Chromatography (UHPLC)-UV-mass spectrometry (MS) on a Thermo Orbitrap Elite coupled with Accela HPLC pump, photodiode array detector, and CTC Leap autoinjector (Thermo Fisher Scientific, Waltham, MA). Separation was effected on an Acquity BEH C18 column (2.1 × 100 mm; 1.7 μm particle size) using a mobile phase consisting of 0.1% formic acid in water (A) and acetonitrile (B) at a flow rate of 0.4 mL/min. The mobile phase composition began at 5% B, held for 0.5 minute, increased linearly to 40% B at 6 minutes, increased linearly to 80% B at 8 minutes, followed by a 1-minute wash at 95% B and 1.5-minute re-equilibration to initial conditions. The effluent passed through the photodiode array detector scanning from 200 to 400 nm and then into the source of the mass spectrometer operated in the positive ion mode. The source temperature was set at 400°C, and other settings and potentials were adjusted to maximize the signal for the protonated molecular ion of imipramine. The injection volume was 10 μL.

Metabolites formed in the hepatocyte incubation of imipramine were identified using UV and total ion chromatograms. The UV chromatograms were reconstructed using the wavelength maxima of the parent compound. These were then compared with UV chromatograms of the corresponding control incubation without parent drug. The UV peaks that were only present in the chromatograms of the incubation mixture but absent in the controls were identified as potential metabolites of imipramine. These were integrated, and the fractional conversion from parent drug (f_m) for desipramine formation from imipramine was estimated as the desipramine peak area divided by the sum of peak areas for all observed imipramine metabolites.

Enzyme Kinetic Study of Imipramine Metabolism in Hepatocytes

A preliminary experiment was conducted to determine linearity with respect to incubation time and hepatocyte concentration, wherein product formation was measured following substrate incubation at several different time points (2–45 minutes) and at several different hepatocyte concentrations (0.25 × 10^6 − 1 × 10^6 cells/mL). For incubation, 30 μL cell suspensions was added to a 96-well polystyrene plate with lid and incubated under a gas mixture of 5% CO_2/95% O_2 for 30 minutes. After preincubation, the reaction was commenced by adding 15 μL imipramine stock solutions prepared in Williams E medium and maintained at 37°C in incubator for 10 minutes. The final hepatocyte concentration was 0.25 × 10^6 cells/mL, and the final substrate concentration ranged from 0.5 to 445 μM. All hepatocyte incubations were quenched by the addition of 135 μL acetonitrile containing internal standard (IS; amitriptyline 0.05 μM), and centrifuged at 3000 rpm for 10 minutes. Supernatant was transferred to a clean 96-well plate for liquid chromatography/tandem mass spectrometry analysis. The experiments were performed in triplicate.

The in vitro data were initially transformed for Eadie-Hofstee plot to assess linearity and diagnose appropriate enzyme kinetic models for the data.

TABLE 2

List of metabolites observed in vitro and corresponding calculated f_m, $f_{CL,m}$

Metabolite	UV Peak Area	f_m	$f_{CL,m}$
Desipramine	45,021	0.44	0.44–0.62
Imipramine N-glucuronide	18,764	0.18	0.18
Hydroxyimipramine	20,339	0.2	0.20–0.38
Hydroxydesipramine	18,498	0.18	
All metabolites	102,622	1	

Kinetic parameters, maximal reaction velocity (V_{max}) and Michaelis-Menten (K_m), were estimated by fitting the selected model to the in vitro data using nonlinear regression in GraphPad Prism (version 6.03).

CL_{int} Determination of Desipramine in CYP2D6 EM and PM Microsomes

The CL_{int} of desipramine was determined in triplicate using HLMs (EM HLMs). Microsomes (0.5 mg/ml) were preincubated for 5 minutes at 37°C in 100 mM KH_2PO_4, pH 7.4, containing 3.3 mM $MgCl_2$, and 1.3 mM NADPH. The reactions were initiated by adding prewarmed test compound (1 μM final concentration of desipramine). After zero, 5, 10, 20, 30, 45, and 60 minutes postcommencement of the incubation, the reactions were stopped by adding a fourfold volume of acetonitrile containing 0.05 μM amitriptyline (IS). The samples were centrifuged at 3000g for 10 minutes. The supernatants were analyzed with liquid chromatography/tandem mass spectrometry for the amount of parent compound remaining.

CL_{int} of desipramine in CYP2D6 PM HLMs using a pool of five CYP2D6 PM donors was determined in similar experimental procedure, except that the incubation mixture included 1 mg/mL pooled PM HLMs.

Calculation of apparent CL_{int} was done using the following equation:

$$CL_{int} = \frac{0.693}{t_{1/2} \times C_{protein}} \times \frac{45 \text{ mg microsomal protein}}{\text{g of liver weight}} \times \frac{20 \text{ g of liver}}{\text{kg body weight}} \quad (1)$$

where $C_{protein}$ is the microsomal protein concentration in the incubation mixture and the in vitro elimination half life ($t_{1/2}$) was determined from the slope (−k) of the linear regression from log percentage remaining versus incubation time relationships ($t_{1/2}$ = −0.693/k).

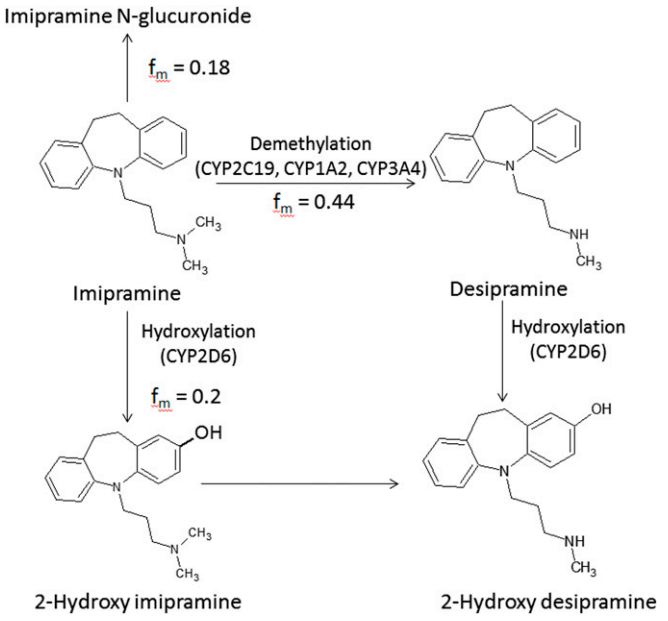

Fig. 2. Proposed pathway of imipramine metabolism and corresponding f_m calculated from HPLC-UV traces of imipramine extracts.

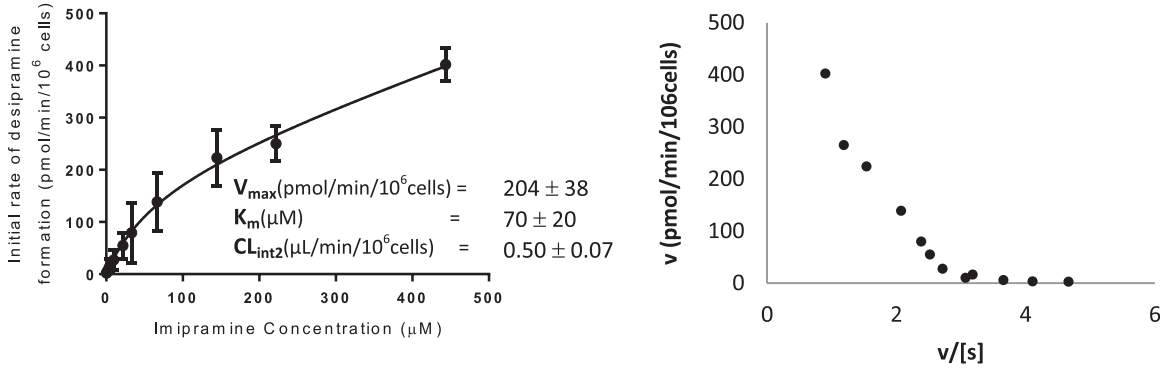

Fig. 3. The formation of desipramine from imipramine in human hepatocytes. Each point represents the mean of triplicate measurements with S.E. bar. Line represents the best fit according to the model expressed by eq. 11. On the right is the Eadie-Hofstee plot of the kinetic data (left) showing that demethylation of imipramine exhibited biphasic kinetics.

CL_{int} Determination of Imipramine in Hepatocytes

Determination of CL_{int} of imipramine in hepatocytes were performed in triplicate, in William E medium, pH 7.4, with final 0.5×10^6 hepatocytes/ml and 1 μM imipramine. The incubations were carried out in a 37°C 5% CO_2/95% O_2 incubator. The reactions were stopped at 0, 5, 15, 30, 60, 120, and 240 minutes with the addition of threefold volume of acetonitrile containing 0.05 μM amitriptyline. The values of 0.5×10^6 hepatocytes/ml and 120×10^6 hepatocytes/g liver for humans (Naritomi et al., 2003) were used in the imipramine CL_{int} calculation (eq. 1).

Protein Binding (Fraction Unbound in Incubation Mixture, Fraction Unbound in Plasma, Fraction Unbound in Hepatocytes)

Microsomes (0.5 mg/mL) were mixed with 1 μM test compound in 100 mM KH_2PO_4, pH 7.4, and $MgCl_2$ (3.3 mM). The mixtures (150 μL) were loaded into the donor compartment of the equilibrium dialysis device. Aliquots of corresponding blank buffer mix (150 μL) were placed into the receiver compartments. Dialysis experiments were performed in quadruplicate. After 4 hours of incubation in an incubator (5% CO_2, 75% relative humidity) on a shaker, the microsomes and buffer samples were removed. Microsomal samples (15 μL) were mixed with control buffer (45 μL), and buffer samples (45 μL) were mixed with control microsomes (15 μL) to yield an identical matrix before samples were precipitated by 180 μL cold acetonitrile containing 0.05 μM amitriptyline (IS). After centrifugation, supernatant was withdrawn for HPLC-MS analysis. Drug recovery and stability through the dialysis procedure were also determined by analyzing samples of the mixtures that were not subjected to dialysis. The fraction unbound in microsomes (fu_{mic}) was calculated from the concentrations of test compound in donor and receiver compartments.

The plasma protein fraction unbound (fu_p) was determined using a similar procedure, except that plasma was thawed and adjusted to pH 7.4 with 1 N HCl before the addition of test compounds.

The fraction unbound in hepatocytes (fu_{cell}) was calculated using eq. 2 reported by Jones et al. (2012), assuming that the concentration of macromolecules (e.g., albumin, globulins, and lipoproteins) in liver relative to that in plasma (Cm_{tissue}/Cm_{plasma}) is equal to 0.5 (Poulin and Theil, 2000).

$$fu_{cell} = \frac{1}{1 + \left(\frac{1 - fu_p}{fu_p}\right) \times \frac{Cm_{tissue}}{Cm_{plasma}}} \quad (2)$$

Prediction of Passive Diffusion Clearance

The rate of total mass transport across a cellular membrane (dM_{pass}/dt) by passive transport can be described by equation below (Sugano et al., 2010):

$$\frac{dM_{pass}}{dt} = A \times P_{pass} \times C \quad (3)$$

where A is the surface area of a membrane (length^2); P is the permeability (length/time); C is the concentration of a permeant (amount/length^3).

Hence, the hepatic passive transport clearance (product of $A \times P_{pass}$) can be predicted from passive permeability and hepatocyte surface area, as follows:

$$CL_{int,pass} = \text{Passive permeability} \times \text{Hepatocyte Cell Surface Area} \times \text{N cells} \quad (4)$$

where passive permeability of desipramine is experimentally measured by parallel artificial membrane permeability assay from Fujikawa et al. (2007) ($P_{PAMPA} = 17.0 \times 10^{-6}$ cm/s). Human hepatocyte cell surface area is 1.6×10^{-5} cm^2 (Chen et al., 2005). Number of cells is the product of 120×10^6 cells/gram liver (Naritomi et al., 2003) and 20 g liver/kg body weight.

Prediction of Metabolite Systemic Availability

Following its formation from imipramine in liver, the systemic availability (F_m) of desipramine was estimated based on the well-stirred model (Houston, 1981), which was modified to incorporate the interplay between passive diffusion, hepatic blood flow (Q_h), and metabolic CL_{int} of desipramine ($CL_{int,u,met}$), assuming no or negligible involvement of hepatic transporters:

$$F_m = \frac{\frac{Q_h \times CL_{int,pass}}{Q_h + CL_{int,pass}}}{\frac{Q_h \times CL_{int,pass}}{Q_h + CL_{int,pass}} + fu_B \times CL_{int,u,met}} \quad (5)$$

where Q_h is ~21 mL/min/kg. The free fraction in blood (fu_B) is the fu_p corrected by the blood-to-plasma ratios, which are 1.02 and 1.16 for imipramine and desipramine, correspondingly obtained as the mean values from resources, including Simcyp library and literature (Ciraulo et al., 1988; Fišar et al., 1996; Obach, 1997, 1999). $CL_{int,pass}$ and $CL_{int,u,met}$ are intrinsic passive diffusion and metabolic clearances, respectively.

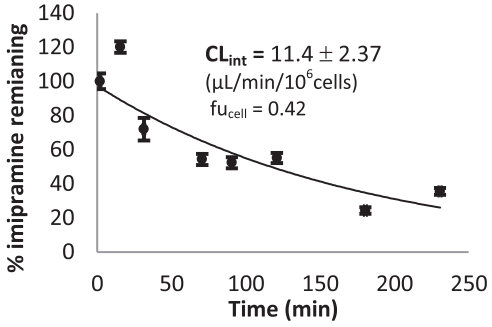

Fig. 4. Percentage of imipramine remaining in hepatocyte incubation (mean values and S.E. bars of triplicate measurements) and fitted exponential depletion curve.

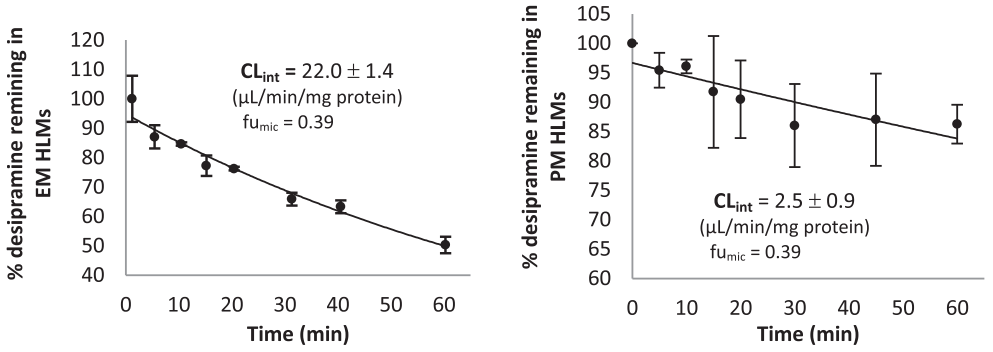

Fig. 5. Percentage of desipramine remaining in EM (left) and PM (right) microsomal incubations (mean values and S.E. bars of triplicate measurements) and fitted exponential depletion curve.

Static Model of AUC_m/AUC_p

The in vivo ratios of area under the plasma concentration-time curve of metabolite versus parent drug after i.v. and oral administration of parent can be described by the following equations (Houston, 1981):

After an i.v. dose of parent drug:

$$\frac{AUC_m}{AUC_p} = \frac{F_m \times f_{CL,m} \times CL_p}{CL_m} \quad (6)$$

After an oral dose of parent drug:

$$\frac{AUC_m}{AUC_p} = \frac{F_m \times f_{CL,m} \times CL_p}{F_h \times CL_m} \quad (7)$$

in which, $f_{CL,m}$ is the fraction of the clearance of the parent drug that yields the metabolite. F_m, the metabolite systemic availability, is the portion of the total metabolite generated within an organ that is released into the systemic circulation before it is either further metabolized or secreted into bile. CL_p is the total clearance of the parent drug, and CL_m is the total clearance of the metabolite. In eq. 7, the fraction of imipramine that escapes first-pass elimination in the liver was estimated from in vitro total clearance of parent:

$$F_h = 1 - \frac{CL_p}{Q_h} \quad (8)$$

In the static model for CYP2D6 EMs, the fraction of imipramine converted to desipramine, $f_{CL,m}$, was estimated based on imipramine metabolic profile determined from EM hepatocyte in vitro system. For PMs, desipramine $f_{CL,m}$ of 0.8 was obtained from clinical data of Brøsen and Gram (1988).

The total body clearance values of parent and metabolite were predicted from in vitro intrinsic metabolic clearances (EM and PM HLM) using the well-stirred model as follows:

$$CL_p = \frac{Q_h \times fu_{B,parent} \times CL_{int,u,parent}}{Q_h + fu_{B,parent} \times CL_{int,u,parent}} \quad (9)$$

$$CL_m = \frac{Q_h \times fu_{B,metab} \times CL_{int,u,metab}}{Q_h + fu_{B,metab} \times CL_{int,u,metab}} \quad (10)$$

PBPK Modeling and Simulations

Modeling and simulations of imipramine and its metabolite desipramine were performed using the population-based ADME simulator Simcyp (version 14; Simcyp, Sheffield, UK). Simulations were performed for two virtual populations of 500 (10 trials × 50 subjects each) healthy volunteers aged between 20 and 50 with a male/female ratio of 50/50, in fasted conditions, representing PM- and EM-CYP2D6 individuals receiving a normalized dose of 1 mg imipramine i.v. or orally. The PM population was generated by setting the frequency of PM CYP2D6 phenotype as 1, and other phenotypes (intermediate metabolizers, ultra-rapid metabolizers, and EM) as 0 in demographic of trial design. Meanwhile, CYP2D6 phenotype PM, IM, and UM frequencies were set to 0 for EM population.

For imipramine, a minimal PBPK model was developed assuming perfusion-limited distribution and using the physicochemical (pKa, logP), biochemical properties (human plasma fu, blood-to-plasma ratio) and in vitro metabolic CL_{int} values (Table 1). The PBPK model for desipramine was similar to its parent drug, using desipramine physicochemical and CL_{int} parameters (Table 1). The volumes of distribution at steady state (V_{ss}) were 11 and 6.5 L/kg, for imipramine and desipramine, respectively. These values were predicted using the model proposed by Rodgers and Rowland (2006). For imipramine metabolism, enzyme kinetic information using in vitro human hepatocytes data was used. The unit of μL/min/10^6 cells was converted to μL/min/mg protein using conversion factors of 120 × 10^6 cells/g liver and 45 mg microsomal protein/g liver (Zhang and Kaminsky, 2008). CL_{int} value of 9.12 μL/min/mg protein for N-demethylation pathway was used after taking the sum of two enzyme kinetic parameters (V_{max}/K_m and CL_{int2}). The value of 8 μL/min/10^6 cells was assigned for additional clearance to account for other pathways by subtracting N-demethylation CL_{int} from total CL_{int} of imipramine. For desipramine metabolism, CL_{int} of 22.0 μL/min/mg protein was assigned to account for hydroxylation pathway by CYP2D6.

HPLC-MS/MS Method for Quantitation of Imipramine and Desipramine

Analyses of substrate and metabolites were performed using HPLC (Agilent model 1290 binary pump), followed by tandem mass spectrometry (Triple Quad 5500; Applied Biosystems/Sciex, Thornhill, Canada). The chromatographic separation was carried out on a Phenomenex Kinetex C18 100Å 30 × 2.1-mm column. Mobile phases consisted of 0.1% formic acid in water (mobile phase A) and 0.1% formic acid in acetonitrile (mobile phase B), and were delivered at 0.5 mL/min. The initial composition of solvent B was maintained at 10% for 0.8 minute, then increased to 90% after 1.2 minutes, and returned to 10% after 1.7 minutes, and held (2.0 minutes total). The injection volume was 10 μL. The TurboIonSpray interface was operated in the positive ion mode at 5500 V and 500°C. Quadrupoles Q1 and Q3 were set on unit resolution. Multiple-reaction–monitoring mode using specific precursor/product ion transitions was used for quantification. Detection of the ions was performed by monitoring the transitions of mass/charge ratio (m/z) with collision energy of 30 eV, as follows: imipramine (281.2→86); desipramine (267→208); and amitriptyline (IS) (278.4→91).

Stock solutions of imipramine, desipramine, and IS (amitriptyline) were prepared in methanol. Desipramine was quantitated from a standard curve ranging from 0.5 to 1000 nM. Data processing was performed using Analyst software (version 1.6.2; Sierra Analytics, Modesto, CA).

Results

Metabolite Profile of Imipramine in Human Hepatocytes to Estimate f_m Values. The metabolism of imipramine was assessed in

TABLE 3

Predicted values for CL_p, CL_m, F_h, $CL_{int,pass}$, and F_m

Substrate	CL_p and CL_m (mL/min/kg)	F_h	$CL_{int,pass}$ (mL/min/kg)	F_m
Imipramine	9.4	0.55	—	—
Desipramine (in EM)	6.4	—	39.1	0.60
Desipramine (in PM)	1.0	—	39.1	0.93

TABLE 4
Predicted AUC ratios

Route	$AUC_{desipramine}/AUC_{imipramine}$					
	CYP2D6 EM Population			CYP2D6 PM Population		
	Static Model	PBPK	Observed	Static Model	PBPK	Observed
Intravenous	0.39–0.54	0.19–0.28	0.21–0.46[a]	7.0	3.7–5.0	
Oral	0.69–0.98	0.32–0.54	0.48–1.1[b]	12.6	6.5–9.1	2.8–6.8[c]

[a]Observed value range was obtained from Sutfin et al. (1984) study, in which single intramuscular doses of imipramine were administered to healthy volunteers.
[b]Abernethy et al., 1984; Sutfin et al., 1984; Brøsen et al., 1986; Wells et al., 1986; Skjelbo et al., 1991; Bergstrom et al., 1992; Koyama et al., 1994; Callaghan et al., 1997; Kurtz et al., 1997; Albers et al., 2000.
[c]Brøsen et al., 1986; Koyama et al., 1994.

human hepatocyte incubations. Chromatograms (UV traces) are shown in Fig. 1, and corresponding fractional conversion from parent drug f_m is listed in Table 2 and Fig. 2. A total of four major metabolites was observed in this in vitro incubation. Primary metabolic pathways of imipramine produced desipramine (m/z 267), hydroxy imipramine (m/z 297), and imipramine N-glucuronide (m/z 457). Hydroxy desipramine may be formed from sequential metabolism of desipramine or demethylation of hydroxy imipramine. Due to this, the fractional conversion from imipramine via N-demethylation pathway ($f_{CL,m}$) was estimated as a range from 0.44 to 0.62. The fraction of imipramine that undergoes hydroxylation is in the range of 0.20–0.38. These ranges reflect extreme cases, that is, that hydroxy desipramine arose 100% via desipramine or 100% via hydroxy imipramine. Glucuronidation is responsible for 0.18 fraction of imipramine metabolism.

Enzyme Kinetic Parameters of Desipramine Formation. The enzyme kinetics of metabolism of imipramine to desipramine was studied in human hepatocytes. The velocity of N-demethylation was investigated using imipramine at final concentrations from 0.5 to 400 μM. The kinetic data are shown in Fig. 3 and indicate that at least two distinct enzymes are responsible for demethylation pathway. The Eadie-Hofstee plot (Fig. 3) showed that demethylation exhibited biphasic kinetics. Therefore, the total velocity for desipramine formation was described by two-enzyme model, as follows:

$$v = \frac{V_{max} \times C}{K_m + C} + CL_{int2} \times C \quad (11)$$

where V_{max} and K_m are the apparent maximal velocity and the apparent Michaelis constant, respectively, of low K_m enzyme, and CL_{int2} is the CL_{int} representing the high K_m site. The best fit values of V_{max}, K_m, and CL_{int2} were shown in Fig. 3.

In Vitro CL_{int} of Imipramine in Hepatocytes and Desipramine in Liver Microsomes. The apparent CL_{int} values of imipramine and its active metabolite, desipramine, were calculated from the degradation rate constants in their corresponding depletion curves (Figs. 4 and 5). For desipramine, HLMs were used because the metabolic clearance of desipramine is mediated mainly by cytochrome P450, whereas for imipramine this measurement was made in human hepatocytes because glucuronidation is also a component of clearance (Nakajima et al., 2002; Zhou et al., 2010). These apparent values were corrected for nonspecific binding of test compounds within microsomal (desipramine fraction unbound in microsomal incubation = 0.39) and hepatocyte (imipramine fu_{cell} = 0.42) incubations. Apparent CL_{int} and protein binding of imipramine and desipramine are displayed in Figs. 4 and 5, respectively. CL_{int} of 2.5 ± 0.9 μL/min/mg protein of desipramine obtained in CYP2D6 PM HLMs was also determined, which is about ninefold lower than the value obtained from EM HLM incubations (22 ± 1.4 μL/min/mg protein). However, this estimate possesses uncertainty because the depletion of desipramine in PM liver microsomes is low.

CL, $CL_{int,pass}$, and F_m Predictions. Table 3 shows the predicted total clearance of parent drug (CL_p) and desipramine (CL_m), hepatic first-pass availability (F_h) of parent drug, as well as intrinsic passive diffusion ($CL_{int,pass}$) and F_m of desipramine. The predicted total clearance of imipramine is 9.4 mL/min/kg, and clearance values of desipramine are 6.4 and 1.0 mL/min/kg for EMs and PMs, respectively. About 55% of imipramine presented in the liver was predicted to escape the first-pass metabolism after an oral dose. Following its formation from imipramine, 60% of desipramine was estimated to leave the liver and reach the systemic circulation in EM populations. Due to its decreased activity of CYP2D6 isozyme in PMs, desipramine elimination rate is decreased, leading to increased systemic availability of this metabolite in circulation (93%) (Table 3).

AUC_m/AUC_p. The predicted total clearance (CL_p and CL_m), f_m, F_h, and F_m were used as input parameters to predict the relative exposure of desipramine compared with parent drug after i.v. and oral administration of imipramine to extensive and PM CYP2D6 healthy populations, using eqs. 6 and 7. For EM populations, the predicted AUC_m/AUC_p ratios are

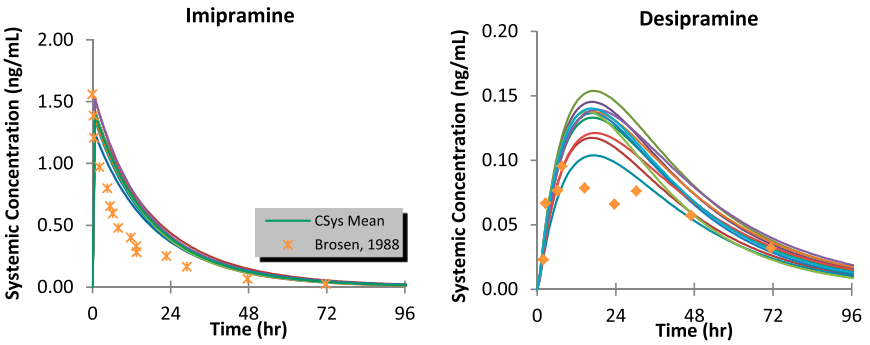

Fig. 6. Simulations of imipramine and desipramine metabolite mean plasma concentration-time profiles after a normalized i.v. dose of 1 mg imipramine in CYP2D6 EM subjects. The points represent 1 mg dose normalized observed mean values. The continuous lines represent the mean predicted values from individual trials (10 × 50; 20–50 years; 50% female).

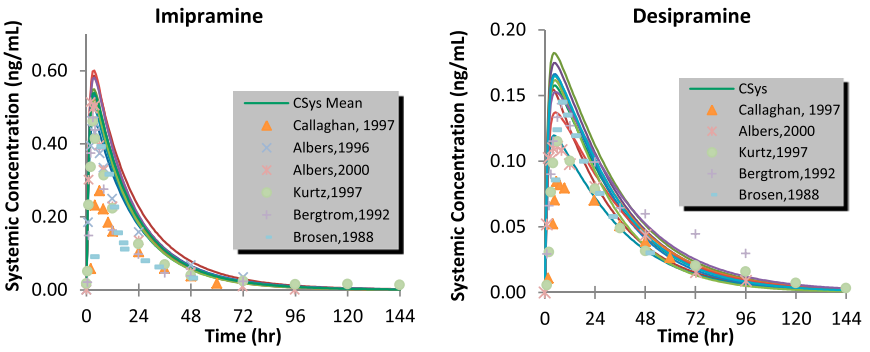

Fig. 7. Simulations of imipramine and desipramine metabolite mean plasma concentration-time profiles after a normalized oral dose of 1 mg imipramine in CYP2D6 EM subjects. The points represent 1 mg dose normalized observed mean values. The continuous lines represent the mean predicted values from individual trials (10 × 50; 20–50 years; 50% female).

consistent with clinical data shown in Table 4. The data highlighted the clinical relevance of the CYP2D6 oxidation polymorphism in the pharmacokinetics of imipramine and desipramine. In the CYP2D6 PMs, increased desipramine plasma levels were predicted when comparing with those in EMs. Due to this, the estimated AUC ratio of desipramine versus imipramine was ~12- to 20-fold higher in PM than in EM populations, following i.v. or oral dosing of parent drug in the static and PBPK models, whereas the observed AUC ratio was 6- to 14-fold higher in PM than in EM volunteers. From PBPK simulations, the predicted mean ratios range from 0.19 to 0.28 and from 0.32 to 0.54 after i.v. and oral dose of imipramine, correspondingly. In PM populations, PBPK model predicted the range of mean ratios from 3.7 to 5.0 and from 6.5 to 9.1 after i.v. and oral dose of imipramine, respectively.

Concentration-Time Profiles of Imipramine and Metabolite Desipramine. The predicted means for 10 trials and observed plasma concentration-time profiles of imipramine and its active metabolite desipramine after i.v. infusion and oral administration of imipramine normalized dose to 1 mg are shown in Figs. 6–9. Predicted PK parameters for imipramine and active metabolite desipramine are listed in Tables 5 and 6. After an oral dose of 1 mg imipramine in EM, mean predicted AUC(0,∞) value of imipramine across the whole population was 13 ng/mL/h, whereas the mean value of individual trial ranged from 12 to 15 ng/mL/h. Mean predicted AUC(0,∞) value of desipramine was 5.8 ng/mL/h (mean of trials ranged from 4.3 to 6.9 ng/mL/h). In CYP2D6 PMs, predicted AUC(0,∞) value of desipramine for the whole population was 104 ng/mL/h (range from 86 to 116 ng/mL/h).

Discussion

Understanding the potential for contribution of a metabolite(s) to drug efficacy, toxicity, or drug-drug interactions can be challenging and requires a thorough knowledge of drug and metabolite disposition. Development of methods to accomplish this requires testing examples of drugs and metabolites that have human pharmacokinetic data and well-understood overall disposition. The example of desipramine as a metabolite which humans are exposed following administration of imipramine was selected for this study because human pharmacokinetics and metabolism are well known. Furthermore, because desipramine is cleared by CYP2D6, this example offers the opportunity to predict desipramine exposure after imipramine administration to two different population groups, that is, CYP2D6 EMs and PMs.

CYP2D6 genes are highly polymorphic, which leads to wide interindividual variation in drug clearance, induction of adverse effects, and increased potential for drug–drug interactions (Bernard et al., 2006). Because desipramine is mainly metabolized by a single enzyme, CYP2D6, it been used widely as a probe drug for CYP2D6 activity (Ball et al., 1997; Kurtz et al., 1997; Spigset et al., 1997; Spina et al., 1997; Madani et al., 2002). High ratios of desipramine to parent drug due to impaired metabolism caused by the CYP2D6 PM phenotype have been related to increased frequency of adverse drug reactions, and even death, upon chronic administration of therapeutic doses (Swanson et al., 1997; Leucht et al., 2000).

In the overall metabolic profile of imipramine (Fig. 2), N-demethylation is the major pathway with the highest fraction of total clearance of the parent drug ($f_{CL,m}$ = 0.44–0.62). Potter et al. (1982) demonstrated a similar finding that desipramine was the major circulating metabolite quantified in patient plasma (accounted for 67% total concentration of metabolites). By measuring the AUCs of desipramine in the PK studies whether desipramine was given as parent compound or formed from imipramine, Brosen et al. (1986) calculated the demethylation fraction of imipramine after the i.v. dose at 0.34 in CYP2D6 EMs and 0.67 in PMs. Likewise, this fraction slightly increased after an oral dose of imipramine: 0.53 in EM and 0.8 in PM populations (Brøsen et al., 1986; Brøsen and Gram, 1988). In CYP2D6 PMs, the decreased activity of CYP2D6 reduces the extent of formation of hydroxyimipramine from imipramine, thereby directing more of the imipramine dose to desipramine, increasing the demethylation fraction of imipramine compared with EM population. By using the HPLC/UV to

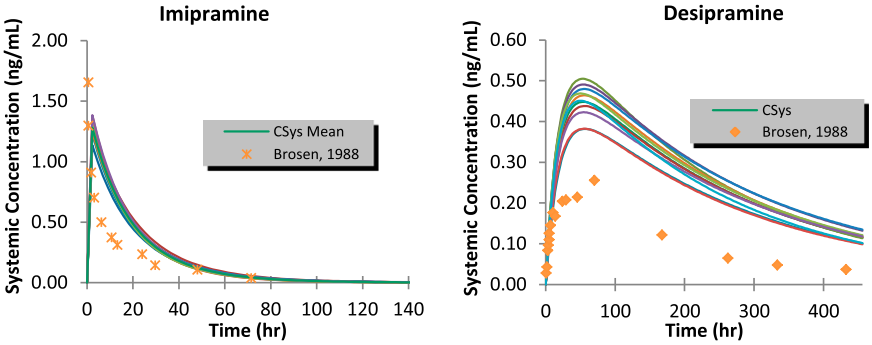

Fig. 8. Simulations of imipramine and desipramine metabolite mean plasma concentration-time profiles after a normalized i.v. dose of 1 mg imipramine in CYP2D6 PM subjects. The points represent 1 mg dose normalized observed mean values. The continuous lines represent the mean predicted values from individual trials (10 × 50; 20–50 years; 50% female).

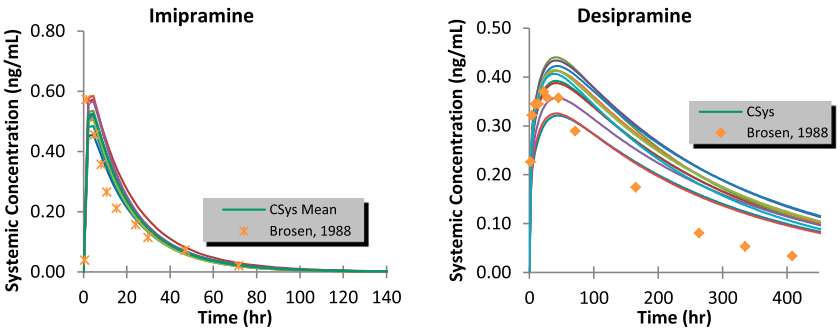

Fig. 9. Simulations of imipramine and desipramine metabolite mean plasma concentration-time profiles after a normalized oral dose of 1 mg imipramine in CYP2D6 PM subjects. The points represent 1 mg dose normalized observed mean values. The continuous lines represent the mean predicted values from individual trials (10 × 50; 20–50 years; 50% female).

determine the fraction of metabolic clearance of parent that forms a specific metabolite, it is acknowledged that in the absence of a standard for the relevant metabolite, assumption of equivalent UV absorptivity needs to be made, even though modifications of the chemical structure can lead to changes in the UV absorbance relative to the parent drug.

To use in vitro data in a bottom-up approach to predict the exposure of a drug metabolite relative to the parent drug exposure, the following parameters must be predicted: total clearance of parent drug (CL_p), total clearance of the metabolite (CL_m), the fraction of the dose of the parent drug that is converted to the metabolite (f_m), and the fraction of the metabolite that once formed can enter the systemic circulation before being cleared within its organ of generation (F_m). The use of in vitro metabolism in scaling to predict human clearance has been a routine practice within pharmaceutical research and development organizations (Obach, 2011). In this study, the predicted CL_p of imipramine of 9.4 mL/min/kg from in vitro CL_{int} was consistent with clinical values ranging from 8 to 15 mL/min/kg (Abernethy et al., 1984; Sutfin et al., 1984; Ciraulo et al., 1988; Sallee and Pollock, 1990). The observed CL_m of desipramine were 2–3 and 12 mL/min/kg in PM and EM populations, respectively (Brøsen and Gram, 1988; Ciraulo et al., 1988), and, in the present study, CL_m of desipramine was reasonably predicted as 1.0 mL/min/kg from in vitro CL_{int} using HLM of PM donors and 6.4 mL/min/kg using EM HLMs. The f_m value was estimated from metabolite profiling experiment, using the UV trace to get an estimate of the percentages. Because there was a secondary metabolite also observed (2-hydroxydesipramine) that could arise via two routes, a range of f_m values was estimated. It is acknowledged that the use of a human hepatocyte metabolite profile has limitations as it does not account for other clearance mechanisms that may occur in vivo (e.g., renal, biliary, extrahepatic metabolism). However, before a new drug candidate can be administered to humans, this method is the best tool available for understanding clearance. In the case of a compound like imipramine, it is reasonable to assume that metabolism will be the clearance mechanism, due to its physicochemical properties (Varma et al., 2015).

Following its formation in liver tissues, desipramine can be subject to sequential metabolism via hydroxylation or permeate the cell membrane into the systemic circulation and the ratio of these two processes will dictate the value F_m. Because a majority of biotransformation reactions result in increased hydrophilicity, metabolites tend to decrease tissue partitioning and plasma protein binding relative to parent drugs (Smith and Obach, 2010; Obach, 2013). In this case, demethylation results in the removal of a methyl group from imipramine, which is a very minor structural change and therefore has a relatively small change in its physicochemical properties. For instance, desipramine exhibits similar lipophilicity (logP of 4.6) as imipramine (logP of 4.8) (Table 1), and this is aligned with the fact that plasma protein binding is not different between imipramine and desipramine, with measured fu_p of 0.26 and 0.21, respectively (Table 6). Desipramine displays high lipoidal permeability similar to its parent drug, and both imipramine and desipramine are rapidly and completely absorbed when taken orally (fraction of a dose absorbed $F_a > 95\%$) (Dencker et al., 1976; Sallee and Pollock, 1990). This high human absorption fraction is correlated with their high passive permeability measured in artificial membrane parallel artificial membrane permeability assay (Avdeef et al., 2007; Chen et al., 2008). Therefore, in this study, the passive diffusion clearance of desipramine from the hepatocyte into the systemic circulation (39.1 mL/min/kg) was deemed to be reasonably predicted from passive permeability and hepatocyte surface area. The estimation of the systemic availability of the metabolite can help to elucidate the currently limited understanding regarding metabolite disposition, that is, the predominant metabolites in vitro are not the same as the predominant metabolites in vivo, or certain metabolites circulate once formed, whereas others do not (Smith and Dalvie, 2012; Zamek-Gliszczynski et al., 2014). These differences can be hypothesized to be associated with metabolic enzymes, as well as basolateral efflux in liver, intestine, and kidney. The availability of desipramine following its formation (F_m) was estimated as 60% (Table 2), which indicates that more than one half of the desipramine generated from imipramine escapes sequential

TABLE 5

Simcyp mean predicted pharmacokinetic parameters of imipramine and desipramine in plasma following i.v. administration of imipramine (normalized dose of 1 mg) in CYP2D6 EM and PM populations

Parameter	Imipramine	Desipramine	
	EM	EM	PM
CL (mL/min/kg)	9.4 (8–15)[a]	—	—
V_{ss} (L/kg)	11 (10–20)[a]	6.5 (10–50)[a]	6.5
AUC (ng/mL/h)	28 (12–22)[a]	6.8 (3.7–6.9)[a]	120

CL, clearance.
[a]Data represented as predicted mean of whole population and range of observed values in parentheses.

TABLE 6

Simcyp mean predicted pharmacokinetic parameters of imipramine and desipramine in plasma following oral administration of imipramine (normalized dose of 1 mg) in CYP2D6 EM and PMs

Parameter	Imipramine	Desipramine	
	EM	EM	PM
C_{max} (ng/mL)	0.46–0.6 (0.35–0.60)[a]	0.12–0.18	0.32–0.42
T_{max} (h)	2.9–3.6 (2.7–5.1)[a]	3.6–5.1	39–46
AUC (ng/mL/h)	12–15 (4.9–10)[a]	4.3–6.9 (4.1–11.2)[a]	86–116
F_h	0.55	—	—
F	0.48 (0.22–0.80)[a]	—	—

[a]Data represented as predicted range of individual trial means and range of observed values in parentheses (Sutfin et al., 1984; Ciraulo et al., 1988; Koyama et al., 1994; Kurtz et al., 1997).

clearance and leaves the liver to enter the systemic circulation. Using all of these values extrapolated from in vitro data, CL_p, CL_m, f_m, and F_m, permitted an estimation of AUC_m/AUC_p for desipramine and imipramine that was in the range observed in clinical studies (Table 4).

The PBPK model built for imipramine was able to simulate the PK profile observed from clinical study following a 50 mg i.v. infusion of imipramine in EM healthy volunteers (Brøsen and Gram, 1988). Both imipramine and desipramine are basic and lipophilic compounds and distribute widely to various tissues. The predicted V_{ss} (11 L/kg) of imipramine using Simcyp is on the low end of reported values mostly ranging from 10 to 20 L/kg (Abernethyl et al., 1984; Ciraulo et al., 1988). The predicted clearance for imipramine is 9.4 mL/min/kg and consistent with the observed range of clinical values (8–15 mL/min/kg). The PBPK model for metabolite desipramine was developed using desipramine in vitro data. Desipramine was predicted to also have a large volume of distribution (V_{ss} = 6.5 L/kg) similar to its parent drug. Based on bottom-up approach with in vitro data as input parameters, the minimal PBPK model captured the shape of desipramine concentration-time curve successfully in both EM and PM populations following oral administration of imipramine (Figs. 7 and 9).

Following oral dosing of imipramine to healthy subjects genotyped as CYP2D6 EMs, the desipramine/imipramine AUC ratio was observed to range from 0.48 to 1.1 (Sutfin et al., 1984; Brøsen and Gram, 1988; Kurtz et al., 1997). Both static and dynamic PBPK models successfully provided AUC_m/AUC_p ratio estimates in reasonable agreement with reported values in EM volunteers. The $AUC_{desipramine}/AUC_{imipramine}$ was about 8 times higher in rapid EM compared with PMs with a long $t_{1/2}$ for desipramine in PM volunteers (more than 2 weeks) (Brøsen et al., 1986). For PM populations, the static and dynamic PBPK models predicted the AUC ratios within twofold of observed values. These findings suggest the relevant impact of CYP2D6 activity on the metabolic disposition of imipramine and that in vitro methods and mechanistic modeling can reasonably predict the relative exposure of active metabolite desipramine. When considering the efficacy of imipramine in depressive patients, imipramine and desipramine concentrations should be taken as a basis for dose recommendation (Kirchheiner et al., 2001).

In conclusion, understanding sequential elimination of major metabolites is important to elucidate metabolite exposure. As shown in the present study, characterization of imipramine and its active metabolite desipramine with respect to metabolic clearance by in vitro methods, binding and membrane permeability properties, all coupled with static and dynamic PBPK models can provide mechanistic insight into overall pharmacokinetics and clinical relevance of genetic polymorphism on exposure to desipramine. The methods described in this work are currently employed to other drug and metabolite pairs wherein overall clearance pathways and dispositional properties are different from the example of imipramine and desipramine.

Acknowledgments

The authors thank Susanna Tse, Manthena Varma, and Jian Lin for insightful suggestions/discussion and software assistance.

Authorship Contributions

Participated in research design: Nguyen, Callegari, Obach.

Conducted experiments: Nguyen, Obach.

Performed data analysis: Nguyen, Callegari, Obach.

Wrote or contributed to the writing of the manuscript: Nguyen, Callegari, Obach.

References

Abernethy DR, Greenblatt DJ, and Shader RI (1984) Imipramine-cimetidine interaction: impairment of clearance and enhanced absolute bioavailability. *J Pharmacol Exp Ther* **229**:702–705.

Abernethyl DR, Divoll M, Greenblatt DJ, Harmatz JS, and Shader RI (1984) Absolute bioavailability of imipramine: influence of food. *Psychopharmacology* **83**:104–106.

Albers LJ, Reist C, Vu RL, Fujimoto K, Ozdemir V, Helmeste D, Poland R, and Tang SW (2000) Effect of venlafaxine on imipramine metabolism. *Psychiatry Res* **96**:235–243.

Avdeef A, Bendels S, Di L, Faller B, Kansy M, Sugano K, and Yamauchi Y (2007) PAMPA: critical factors for better predictions of absorption. *J Pharm Sci* **96**:2893–2909.

Ball SE, Ahern D, Scatina J, and Kao J (1997) Venlafaxine: in vitro inhibition of CYP2D6 dependent imipramine and desipramine metabolism; comparative studies with selected SSRIs, and effects on human hepatic CYP3A4, CYP2C9 and CYP1A2. *Br J Clin Pharmacol* **43**: 619–626.

Bergstrom RF, Peyton AL, and Lemberger L (1992) Quantification and mechanism of the fluoxetine and tricyclic antidepressant interaction. *Clin Pharmacol Ther* **51**:239–248.

Bernard S, Neville KA, Nguyen AT, and Flockhart DA (2006) Interethnic differences in genetic polymorphisms of CYP2D6 in the U.S. population: clinical implications. *Oncologist* **11**: 126–135.

Brøsen K and Gram LF (1988) First-pass metabolism of imipramine and desipramine: impact of the sparteine oxidation phenotype. *Clin Pharmacol Ther* **43**:400–406.

Brøsen K, Otton SV, and Gram LF (1986) Imipramine demethylation and hydroxylation: impact of the sparteine oxidation phenotype. *Clin Pharmacol Ther* **40**:543–549.

Callaghan JT, Cerimele BJ, Kassahun KJ, Nyhart EH, Jr, Hoyes-Beehler PJ, and Kondraske GV (1997) Olanzapine: interaction study with imipramine. *J Clin Pharmacol* **37**:971–978.

Callegari E, Kalgutkar AS, Leung L, Obach RS, Plowchalk DR, and Tse S (2013) Drug metabolites as cytochrome p450 inhibitors: a retrospective analysis and proposed algorithm for evaluation of the pharmacokinetic interaction potential of metabolites in drug discovery and development. *Drug Metab Dispos* **41**:2047–2055.

Chen M, Tabaczewski P, Truscott SM, Van Kaer L, and Stroynowski I (2005) Hepatocytes express abundant surface class I MHC and efficiently use transporter associated with antigen processing, tapasin, and low molecular weight polypeptide proteasome subunit components of antigen processing and presentation pathway. *J Immunol* **175**:1047–1055.

Chen X, Murawski A, Patel K, Crespi CL, and Balimane PV (2008) A novel design of artificial membrane for improving the PAMPA model. *Pharm Res* **25**:1511–1520.

Ciraulo DA, Barnhill JG, and Jaffe JH (1988) Clinical pharmacokinetics of imipramine and desipramine in alcoholics and normal volunteers. *Clin Pharmacol Ther* **43**:509–518.

Dahl M-L, Johansson I, Palmertz MP, Ingelman-Sundberg M, and Sjöqvist F (1992) Analysis of the CYP2D6 gene in relation to debrisoquin and desipramine hydroxylation in a Swedish population. *Clin Pharmacol Ther* **51**:12–17.

Dencker H, Dencker SJ, Green A, and Nagy A (1976) Intestinal absorption, demethylation, and enterohepatic circulation of imipramine. *Clin Pharmacol Ther* **19**:584–586.

European Medicines Agency (2012) Guideline on the investigation of drug interactions. *Committee for Human Medicinal Products (CHMP)*, London.

Food and Drug Administration (2012) *Guidance for industry: drug interaction studies-study design, data analysis, implications for dosing, and labeling recommendations*. Center for Drug Evaluation and Research (CDER), Rockville.

Fišar Z, Krulík R, Fuksová K, and Sikora J (1996) Imipramine distribution among red blood cells, plasma and brain tissue. *Gen Physiol Biophys* **15**:51–64.

Fujikawa M, Nakao K, Shimizu R, and Akamatsu M (2007) QSAR study on permeability of hydrophobic compounds with artificial membranes. *Bioorg Med Chem* **15**:3756–3767.

Furman KD, Grimm DR, Mueller T, Holley-Shanks RR, Bertz RJ, Williams LA, Spear BB, and Katz DA (2004) Impact of CYP2D6 intermediate metabolizer alleles on single-dose desipramine pharmacokinetics. *Pharmacogenetics* **14**:279–284.

Houston JB (1981) Drug metabolite kinetics. *Pharmacol Ther* **15**:521–552.

Houston JB and Taylor G (1984) Drug metabolite concentration-time profiles: influence of route of drug administration. *Br J Clin Pharmacol* **17**:385–394.

ICH (2009) *Guidance on nonclinical safety studies for the conduct of human clinical trials and marketing authorization for pharmaceuticals M3 (R2)*, International Council on Harmonisation of Technical Requirements for Registration of Pharmaceuticals for Human Use, Geneva.

Jamei M, Dickinson GL, and Rostami-Hodjegan A (2009) A framework for assessing inter-individual variability in pharmacokinetics using virtual human populations and integrating general knowledge of physical chemistry, biology, anatomy, physiology and genetics: a tale of 'bottom-up' vs 'top-down' recognition of covariates. *Drug Metab Pharmacokinet* **24**:53–75.

Jones HM, Barton HA, Lai Y, Bi YA, Kimoto E, Kempshall S, Tate SC, El-Kattan A, Houston JB, Galetin A, et al. (2012) Mechanistic pharmacokinetic modeling for the prediction of transporter-mediated disposition in humans from sandwich culture human hepatocyte data. *Drug Metab Dispos* **40**:1007–1017.

Kirchheiner J, Brøsen K, Dahl M-L, Gram LF, Kasper S, Roots I, Sjöqvist F, Spina E, and Brockmöller J (2001) CYP2D6 and CYP2C19 genotype-based dose recommendations for antidepressants: a first step towards subpopulation-specific dosages. *Acta Psychiatr Scand* **104**: 173–192.

Koyama E, Sohn D-R, Shin S-G, Chiba K, Shin J-G, Kim Y-H, Echizen H, and Ishizaki T (1994) Metabolic disposition of imipramine in oriental subjects: relation to metoprolol alpha-hydroxylation and S-mephenytoin 4′-hydroxylation phenotypes. *J Pharmacol Exp Ther* **271**: 860–867.

Kurtz DL, Bergstrom RF, Goldberg MJ, and Cerimele BJ (1997) The effect of sertraline on the pharmacokinetics of desipramine and imipramine. *Clin Pharmacol Ther* **62**:145–156.

Leucht S, Hackl H-J, Steimer W, Angersbach D, and Zimmer R (2000) Effect of adjunctive paroxetine on serum levels and side-effects of tricyclic antidepressants in depressive inpatients. *Psychopharmacology* **147**:378–383.

Madani S, Barilla D, Cramer J, Wang Y, and Paul C (2002) Effect of terbinafine on the pharmacokinetics and pharmacodynamics of desipramine in healthy volunteers identified as cytochrome P450 2D6 (CYP2D6) extensive metabolizers. *J Clin Pharmacol* **42**:1211–1218.

Mahar Doan KM, Humphreys JE, Webster LO, Wring SA, Shampine LJ, Serabjit-Singh CJ, Adkison KK, and Polli JW (2002) Passive permeability and P-glycoprotein-mediated efflux differentiate central nervous system (CNS) and non-CNS marketed drugs. *J Pharmacol Exp Ther* **303**:1029–1037.

Nakajima M, Tanaka E, Kobayashi T, Ohashi N, Kume T, and Yokoi T (2002) Imipramine N-glucuronidation in human liver microsomes: biphasic kinetics and characterization of UDP-glucuronosyltransferase isoforms. *Drug Metab Dispos* **30**:636–642.

Naritomi Y, Terashita S, Kagayama A, and Sugiyama Y (2003) Utility of hepatocytes in predicting drug metabolism: comparison of hepatic intrinsic clearance in rats and humans in vivo and in vitro. *Drug Metab Dispos* **31**:580–588.

Nguyen HQ, Kimoto E, Callegari E, and Obach RS (2016) Mechanistic modeling to predict midazolam metabolite exposure from in vitro data. *Drug Metab Dispos* **44**:781–791.
Obach RS (1997) Nonspecific binding to microsomes: impact on scale-up of in vitro intrinsic clearance to hepatic clearance as assessed through examination of warfarin, imipramine, and propranolol. *Drug Metab Dispos* **25**:1359–1369.
Obach RS (1999) Prediction of human clearance of twenty-nine drugs from hepatic microsomal intrinsic clearance data: an examination of in vitro half-life approach and nonspecific binding to microsomes. *Drug Metab Dispos* **27**:1350–1359.
Obach RS (2011) Predicting clearance in humans from in vitro data. *Curr Top Med Chem* **11**: 334–339.
Obach RS (2013) Pharmacologically active drug metabolites: impact on drug discovery and pharmacotherapy. *Pharmacol Rev* **65**:578–640.
Pang KS (1985) A review of metabolite kinetics. *J Pharmacokinet Biopharm* **13**:633–662.
Potter WZ, Calil HM, Sutfin TA, Zavadil AP, 3rd, Jusko WJ, Rapoport J, and Goodwin FK (1982) Active metabolites of imipramine and desipramine in man. *Clin Pharmacol Ther* **31**:393–401.
Poulin P and Theil FP (2000) A priori prediction of tissue:plasma partition coefficients of drugs to facilitate the use of physiologically-based pharmacokinetic models in drug discovery. *J Pharm Sci* **89**:16–35.
Rodgers T and Rowland M (2006) Physiologically based pharmacokinetic modelling 2: predicting the tissue distribution of acids, very weak bases, neutrals and zwitterions. *J Pharm Sci* **95**:1238–1257.
Rowland M, Peck C, and Tucker G (2011) Physiologically-based pharmacokinetics in drug development and regulatory science. *Annu Rev Pharmacol Toxicol* **51**:45–73.
Sallee FR and Pollock BG (1990) Clinical pharmacokinetics of imipramine and desipramine. *Clin Pharmacokinet* **18**:346–364.
Schenk PW, van Fessem MA, Verploegh-Van Rij S, Mathot RA, van Gelder T, Vulto AG, van Vliet M, Lindemans J, Bruijn JA, and van Schaik RH (2008) Association of graded allele-specific changes in CYP2D6 function with imipramine dose requirement in a large group of depressed patients. *Mol Psychiatry* **13**:597–605.
Skjelbo E, Brøsen K, Hallas J, and Gram LF (1991) The mephenytoin oxidation polymorphism is partially responsible for the N-demethylation of imipramine. *Clin Pharmacol Ther* **49**:18–23.
Smith DA and Dalvie D (2012) Why do metabolites circulate? *Xenobiotica* **42**:107–126.
Smith DA and Obach RS (2010) Metabolites: have we MIST out the importance of structure and physicochemistry? *Bioanalysis* **2**:1223–1233.
Spigset O, Granberg K, Hägg S, Norström A, and Dahlqvist R (1997) Relationship between fluvoxamine pharmacokinetics and CYP2D6/CYP2C19 phenotype polymorphisms. *Eur J Clin Pharmacol* **52**:129–133.
Spina E, Gitto C, Avenoso A, Campo GM, Caputi AP, and Perucca E (1997) Relationship between plasma desipramine levels, CYP2D6 phenotype and clinical response to desipramine: a prospective study. *Eur J Clin Pharmacol* **51**:395–398.
St-Pierre MV, Xu X, and Pang KS (1988) Primary, secondary, and tertiary metabolite kinetics. *J Pharmacokinet Biopharm* **16**:493–527.
Sugano K, Kansy M, Artursson P, Avdeef A, Bendels S, Di L, Ecker GF, Faller B, Fischer H, Gerebtzoff G, et al. (2010) Coexistence of passive and carrier-mediated processes in drug transport. *Nat Rev Drug Discov* **9**:597–614.
Sutfin TA, DeVane CL, and Jusko WJ (1984) The analysis and disposition of imipramine and its active metabolites in man. *Psychopharmacology* **82**:310–317.
Swanson JR, Jones GR, Krasselt W, Denmark LN, and Ratti F (1997) Death of two subjects due to imipramine and desipramine metabolite accumulation during chronic therapy: a review of the literature and possible mechanisms. *J Forensic Sci* **42**:335–339.
Varma MV, Steyn SJ, Allerton C, and El-Kattan AF (2015) Predicting clearance mechanism in drug discovery: extended clearance classification system (ECCS). *Pharm Res* **32**:3785–3802.
Vieira MD, Kim MJ, Apparaju S, Sinha V, Zineh I, Huang SM, and Zhao P (2014) PBPK model describes the effects of comedication and genetic polymorphism on systemic exposure of drugs that undergo multiple clearance pathways. *Clin Pharmacol Ther* **95**:550–557.
Wells BG, Pieper JA, Self TH, Stewart CF, Waldon SL, Bobo L, and Warner C (1986) The effect of ranitidine and cimetidine on imipramine disposition. *Eur J Clin Pharmacol* **31**:285–290.
Yeung CK, Fujioka Y, Hachad H, Levy RH, and Isoherranen N (2011) Are circulating metabolites important in drug-drug interactions? Quantitative analysis of risk prediction and inhibitory potency. *Clin Pharmacol Ther* **89**:105–113.
Yu H and Tweedie D (2013) A perspective on the contribution of metabolites to drug-drug interaction potential: the need to consider both circulating levels and inhibition potency. *Drug Metab Dispos* **41**:536–540.
Zamek-Gliszczynski MJ, Chu X, Polli JW, Paine MF, and Galetin A (2014) Understanding the transport properties of metabolites: case studies and considerations for drug development. *Drug Metab Dispos* **42**:650–664.
Zhang Z and Kaminsky LS (2008) Determination of metabolic rates and enzyme kinetics, in *Drug Metabolism in Drug Design and Development* (Zhang D, Zhu M, and Humphreys WG eds) pp 413–441, John Wiley & Sons, Hoboken.
Zhou D, Guo J, Linnenbach AJ, Booth-Genthe CL, and Grimm SW (2010) Role of human UGT2B10 in N-glucuronidation of tricyclic antidepressants, amitriptyline, imipramine, clomipramine, and trimipramine. *Drug Metab Dispos* **38**:863–870.

Address correspondence to: Dr. Hoa Q. Nguyen, Department of Drug Metabolism and Pharmacokinetics, R&D 1521, Boehringer Ingelheim, 900 Ridgebury Road, Ridgefield, CT 06877. E-mail: hoa_2.nguyen@boehringer-ingelheim.com